Battery Management System Based on Battery Nonlinear Dynamics Modeling

Antoni Szumanowski and Yuhua Chang

***Abstract*—This paper presents a method of determining electromotive force and battery internal resistance as time functions, which are depicted as functions of state of charge (SOC) because SOC $= f(t)$. The model is based on battery discharge and charge characteristics under different constant currents that are tested by a laboratory experiment. This paper further presents the method of determining the battery SOC according to a battery modeling result. The influence of temperature on battery performance is analyzed according to laboratory-tested data, and the theoretical background for calculating the SOC is obtained. The algorithm of battery SOC indication is depicted in detail. The algorithm of the battery SOC "online" indication considering the influence of temperature can be easily used in practice by a microprocessor. An NiMH battery is used in this paper to depict the modeling method. In fact, the method can also be used for different types of contemporary batteries, as well as Li-ion batteries, if the required test data are available.**

***Index Terms*—Battery modeling, electromotive force (EMF), hybrid electric vehicle (HEV), internal resistance, simulation.**

I. Introduction

HYBRID electric vehicles (HEVs) are remarkable solutions for the worldwide environmental and energy problem caused by automobiles. The research and development of various technologies in HEVs is being actively conducted [1]–[8]. The role of the battery as the power source in HEVs is significant. Dynamic nonlinear modeling and simulations are the only tools for the optimal adjustment of battery parameters according to analyzed driving cycles. The battery's capacity, voltage, and mass should be minimized, considering its overload currents. This is the way to obtain the minimum cost of the battery according to the demands of its performance, robustness, and operating life.

The process of battery adjustment and its management is crucial during hybrid drive design. This paper presents the generic model of an electrochemical accumulator, which can be used in every type of battery. This generic model is based on physical and mathematical modeling of the fundamental electrical impacts during energy conservation by a battery. The model is oriented to the calculation of the parameters electromotive force (EMF) and internal resistance. It is easy to find the direct relations between the state of charge (SOC) and these two parameters. If the EMF is defined, and the function versus the SOC ($k \in \langle 0, 1 \rangle$) is known, it is simple to depict the discharge/charge state of a battery. The model is really nonlinear because the correlative parameters of equations are functions of time [or functions of the SOC because SOC $= f(t)$] during battery operation. The modeling method presented in this paper must use the laboratory data (for instance, voltage for different constant currents or internal resistance versus the battery SOC) that are expressed in a static form. These data must be obtained in discharging and charging tests. The considered generic model is easily adapted to different types of battery data and is expressed in a dynamic way using approximation and iteration methods.

An HEV operation puts unique demands on a battery when it operates as the auxiliary power source. To optimize its operating life, the battery must spend minimal time in overcharge and/or overdischarge. The battery must be capable of furnishing or absorbing large currents almost instantaneously while operating from a partial-state-of-charge baseline of roughly 50% [9]. For this reason, knowledge about battery internal loss (efficiency) is significant, which influences the battery SOC. There are many studies that are dedicated to determining the battery SOC [10]–[22]; however, these solutions have some limitations for practical application [23]. Some solutions for practical application are based on a loaded terminal voltage [17]–[20] or a simple calculation of the flow of charge to/from a battery [21], [22], which is the integral that is based on current and time. Both solutions are not considered strong nonlinear behavior of a battery. It is possible to determine the transitory value of the SOC "online" in real drive conditions with proper accuracy, considering the nonlinear characteristic of a battery by resolving the mathematical model that is presented in this paper.

This is the background for optimal battery parameters as well as the proper battery management system design—particularly in the case of the SOC indication. In this paper, the high-power (HP) NiMH battery, which is so commonly used in HEVs, was considered. The method can be also used for different types of contemporary batteries, as well as Li-ion batteries [8], [24], if the required test data are available.

Manuscript received September 19, 2006; revised June 21, 2007, July 26, 2007, and September 13, 2007. The review of this paper was coordinated by Prof. A. Emadi.

The authors are with Warsaw University of Technology, 00-661 Warsaw, Poland (e-mail: asz@simr.pw.edu.pl; yuhua.chang@simr.pw.edu.pl).

Color versions of one or more of the figures in this paper are available online at http://ieeexplore.ieee.org.

Digital Object Identifier 10.1109/TVT.2007.912176

II. Battery Dynamic Modeling

A. Battery Physical Model

The basis enabling the formulation of the energy model of an electrochemical battery is the battery physical model shown in Fig. 1.

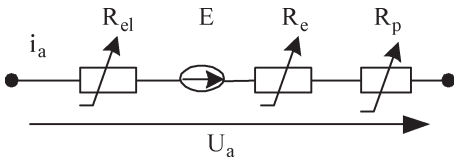

Fig. 1. Substitute circuit for nonlinear battery modeling.

B. Mathematical Modeling

The internal resistance can be expressed in an analytical way [7], where

$$R_w(i_a,\tau,Q) = R_{el}(\tau,Q) + R_e(Q) + bE(i_a,\tau,Q)I_a^{-1} \quad (1)$$

$bE(i_a,\tau,Q)I_a^{-1}$ is the resistance of polarization.

b is the coefficient that expresses the relative change of the polarization's EMF on the cell's terminals during the flow of the I_a current in relation to the EMF E for nominal capacity. Electrolyte resistance R_{el} and electrode resistance R_e are inversely proportional to the temporary capacity of the battery. During real operation, the capacity of the battery is changeable with respect to current and temperature [7], i.e.,

$$Q_u(i_a,t,\tau) = Q_\tau(\tau) - K_w\left(i_a(t),t\right) \quad (2)$$

or

$$Q_u(i_a,t,\tau) = Q_\tau(\tau,i_a) - \int_0^t i_a(t)dt \quad (3)$$

where $K_w(i_a(t),t)$ is the nonlinear function that is used to calculate the battery discharged capacity, $\int_0^t i_a(t)dt$ is the function that is used to calculate the used charge, which has been drawn from the battery since the instant time $t=0$ until the time t, $Q_\tau(\tau,i_a)$ is the battery capacity as a function of temperature and load current, and

$$K_w = i_a^{n(\tau)}t \quad (4)$$

where K_w is the discharge capacity of the battery, and n is the Peukert's constant, which varies for different types of batteries.

Assume the temperature influence

$$Q_u(i,t,\tau) = c_\tau(\tau)Q_{\tau n}\left(\frac{i_a(t)}{I_n}\right)^{-\beta} - \int_0^t i_a(t)dt \quad (5)$$

where the $c_\tau(\tau)$ coefficient can be defined as the temperature index of nominal capacity [7], i.e.,

$$c_\tau(\tau) = \frac{Q_\tau}{Q_{\tau n}} = \frac{1}{1+\alpha\left|(\tau_n-\tau)\right|} \quad (6)$$

where α is the temperature capacity index (we can assume that $\alpha \approx 0.01\ \deg^{-1}$).

According to the Peukert equation, we can obtain the following:

$$\frac{Q(i_a)\overline{U}}{Q_{\tau n}\overline{U}} = \left(\frac{i_a(t)}{I_n}\right)^{-\beta(\tau)}. \quad (7)$$

The left-hand side of (7) is the quotient of the electric power that is drawn from the battery during the flow of $i_a \neq I_n$ current and the electric power that is drawn from the battery during loading with the rated current. The quotient mentioned above defines the usability index of the accumulated power, i.e.,

$$\eta_A(i_a,\tau) = \left(\frac{i_a(t)}{I_n}\right)^{-\beta(\tau)}. \quad (8)$$

When $i_a < I_n$, the value of the index can exceed 1.

During further solution of (5), it can be transformed by means of (8), i.e.,

$$Q_u(i,t,\tau) = c_\tau(\tau)\eta_A(i_a,\tau)Q_{\tau n} - \int_0^t i_a(t)dt. \quad (9)$$

Therefore, the real battery SOC can be expressed in the following way [7]:

$$k = \frac{Q_u}{Q_{\tau n}} = \frac{c_\tau(\tau)\eta_A(i_a,\tau)Q_{\tau n} - \int_0^t i_a(t)dt}{Q_{\tau n}} \quad (10)$$

where $k=1$ for a nominally charged battery, $0 \le k \le 1$, and thus

$$k = c_\tau(\tau)\eta_A(i_a,\tau) - \frac{1}{Q_{\tau n}}\int_0^t i_a(t)dt. \quad (11)$$

For practical application, it is necessary to transform the aforementioned equations for determining the internal resistance R_w and the EMF as functions of k (SOC) [7], i.e.,

$$R_w(i_a,\tau,Q) = \frac{l_1}{Q_u(i_a,t,\tau)} + \frac{l_2}{Q_u(i_a,t,\tau)} + \frac{bE(i_a,\tau,Q)}{i_a(t)} \quad (12)$$

$$R_w(i_a,t,\tau) = lk^{-1} + b\frac{E(k)}{i_a(t)} \quad (13)$$

where $l = (l_1+l_2)Q_{\tau n}^{-1}$, and $l \approx$ const is a piecewise constant, assuming that the temporary change of the battery capacity is significantly smaller than its nominal capacity; the coefficient l is experimentally determined under static conditions. $E(k)$ is a temporary value of the polarization's EMF, which is dependent on the SOC.

The EMF as a function of k is deduced from the well-known battery voltage equation, including the momentary value of voltage and internal resistance, because the values R_w and EMF are unknown. A solution can be obtained by a linearization and iterative method, which is explained by Fig. 2 and by the following:

$$b(k) = \frac{E(k) - E^*_{\min}}{E^*_{\max}}. \quad (14)$$

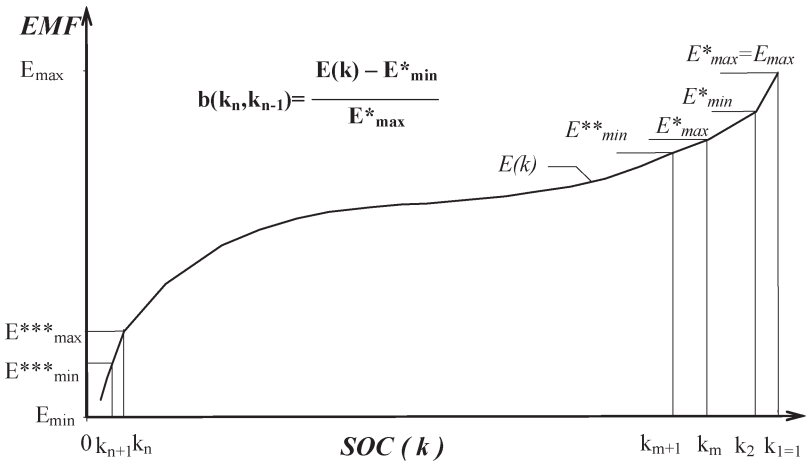

Fig. 2. Linearization method of EMF versus SOC (k).

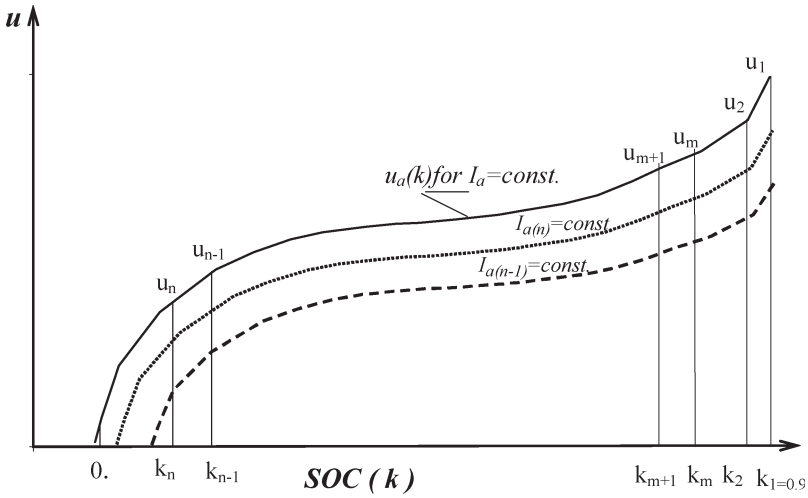

Fig. 3. Linearization method of voltage versus SOC (k).

Take under consideration (12)–(14). It is then possible to obtain the following:

$$\begin{cases} R_w(k_n) = \frac{E(k_n)-E^*_{\min}}{E^*_{\max}} \frac{E(k_n)}{I_n} + \frac{l(k_n)}{k_n} \\ R_w(k_{n-1}) = \frac{E(k_{n-1})-E^*_{\min}}{E^*_{\max}} \frac{E(k_{n-1})}{I_n} + \frac{l(k_{n-1})}{k_{n-1}}. \end{cases} \tag{15}$$

Obviously, $E(k)$ is the function that we need. To obtain it, it is necessary to use the known functions $u_a(k)$, which are obtained by laboratory tests.

Similarly as in the case of Fig. 3, the following equations are generated:

$$\begin{cases} u(k_n) = E(k_n) \pm I_a R_w(k_n) \\ u(k_{n-1}) = E(k_{n-1}) \pm I_a R_w(k_{n-1}). \end{cases} \tag{16}$$

$u(k_n)$ and $u(k_{n-1})$ are known from the family of voltage characteristics that are obtained by laboratory tests. $I_{a(n)}$ is also known because $u(k_n)$ is determined for $I_{a(n)} = \text{const}$.

$+$ is for discharge.
$-$ is for charge.
$k \in \langle 0, 1 \rangle$.

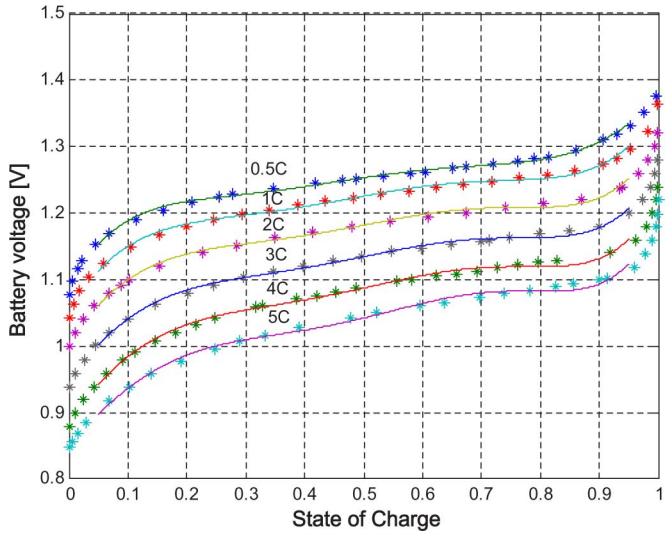

Fig. 4. Discharging data of a 14-Ah NiMH battery.

Using the above-presented approach, based on experimental data (shown in Figs. 4 and 5), it is possible to construct a proper equation set as in the shape of (15) and (16) and resolve it in an iterative way.

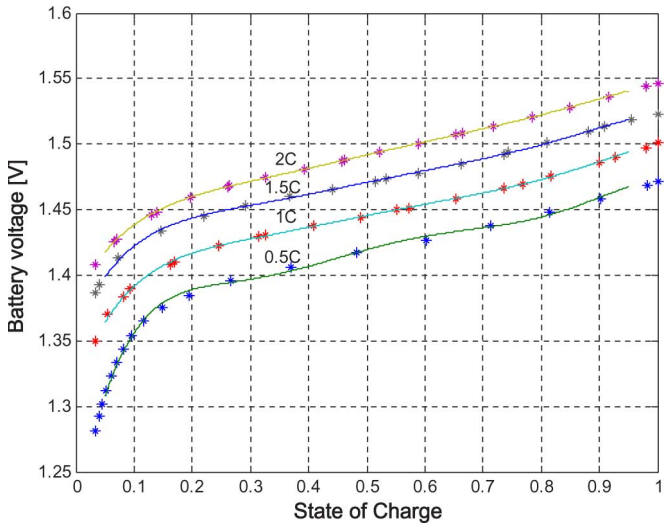

Fig. 5. Charging data of a 14-Ah NiMH battery.

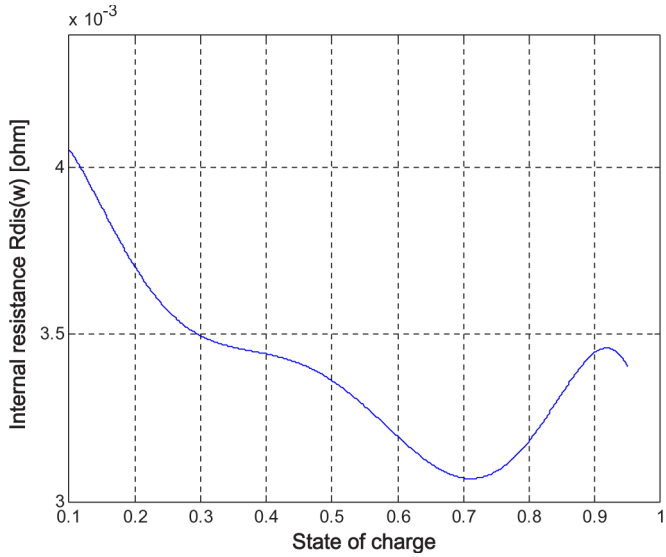

Fig. 6. Computed internal resistance characteristics of a 14-Ah NiMH battery for discharging.

Last, the equations of R_w and EMF take the shape of the following polynomial:

$$\begin{aligned} R_w(k) &= A_r k^6 + B_r k^5 + C_r k^4 + D_r k^3 \\ &\quad + E_r k^2 + F_r k + G_r \\ E(k) &= A_e k^6 + B_e k^5 + C_e k^4 + D_e k^3 \\ &\quad + E_e k^2 + F_e k + G_e \\ b(k) &= A_b k^6 + B_b k^5 + C_b k^4 + D_b k^3 \\ &\quad + E_b k^2 + F_b k + G_b \\ l(k) &= A_l k^7 + B_l k^6 + C_l k^5 + D_l k^4 \\ &\quad + E_l k^3 + F_l k^2 + G_l k + H_l. \end{aligned} \tag{17}$$

III. Battery Modeling Results

The basic elements that are used to formulate the mathematical model of an NiMH battery are the described iteration–approximation method and the approximations based on battery discharging and charging characteristics that are obtained by an experiment. Experimental data are approximated

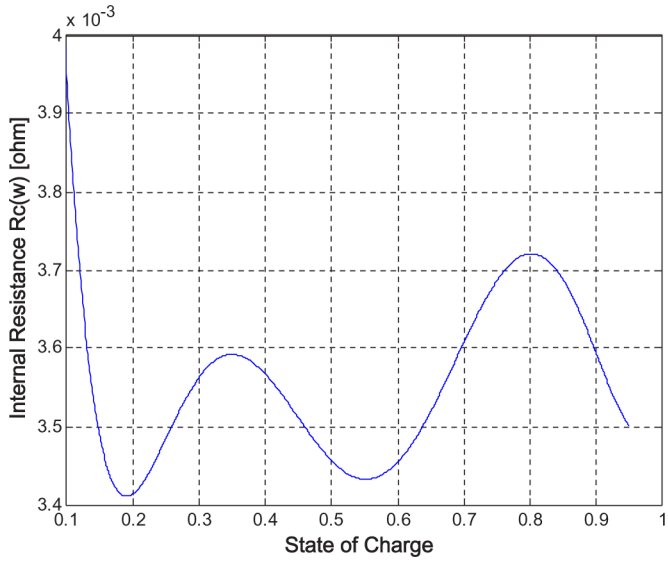

Fig. 7. Computed internal resistance characteristics of a 14-Ah NiMH battery for charging.

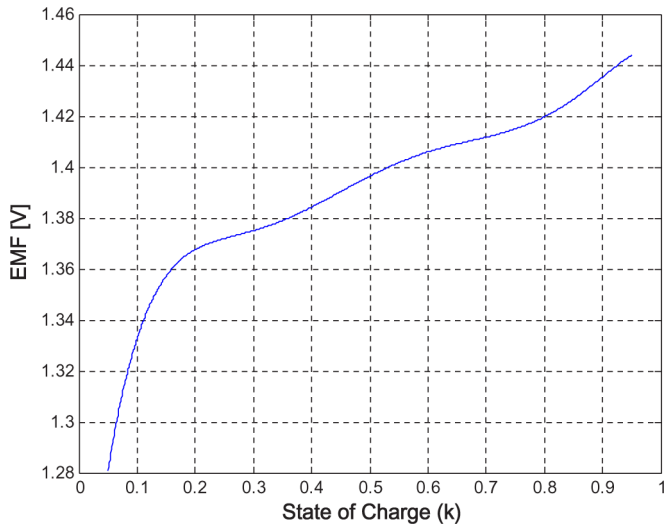

Fig. 8. Computed EMF of a 14-Ah NiMH battery.

to enable determination of the internal resistance in a small-enough range $k = 0.001$. The modeling results (Figs. 6–8) in the battery SOC operating range of 0.1–0.95 show a small deviation (less than 1%) from the experimental data (Figs. 9 and 10). The NiMH battery that is used in the experiment and the modeling is an HP battery for HEV application. The nominal voltage of the battery is 1.2 V, and the rated capacity is 14 Ah.

After the approximation according to the computed results, approximated equations of (17) can be obtained. These factors of (17) are available in Table I.

IV. Temperature Influence Analysis on Battery Performance

The determination of the battery EMF and internal resistance gives unlimited possibilities of calculating the battery's voltage versus SOC (k) relation for a different value of discharge–charge current. For a real driving condition, the battery discharge or charge depends on the drive architecture influencing the respective power distribution. In majority,

TABLE I
FACTORS OF (17)

Factor	Internal resistance R(w) during discharge	Internal resistance Rd(w) during charge	EMF	Coefficient b	Coefficient l
				discharge	discharge
				charge	charge
A	0.65917	0.42073	13.504	-0.015363	0.65917
				0.015341	0.42073
B	-2.0397	-1.4434	-36.406	0.10447	-2.0528
				-0.10661	-1.4376
C	2.4684	1.9362	36.881	-0.18433	2.4978
				0.22702	1.9195
D	-1.4711	-1.2841	-17.198	0.13578	-1.495
				-0.21788	-1.2661
E	0.44578	0.43809	3.5264	-0.045129	0.45416
				0.10346	0.42896
F	-0.065274	-0.071757	-0.1079	0.0059814	-0.066422
				-0.023367	-0.06961
G	0.009911	0.007	1.234	-9.416e-5	0.0099289
				0.0020389	0.0076585
H					-1.2154e-015
					1.9984e-008

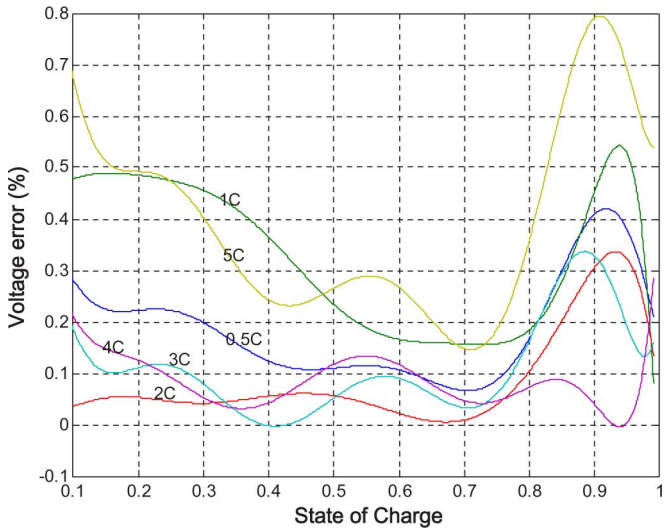

Fig. 9. Error of experiment data and the computed voltage at different discharge currents.

battery charging takes place during vehicle regenerative braking, which means that this situation lasts for a relatively short time with a significant peak-current value. A discharging current that is too high results in a rapid increase in the battery temperature.

The main role of this study is to find a theoretical background for calculating the temperature influence on the battery SOC. The presented method is more accurate and complicated compared with other methods, which does not mean that it is more difficult to apply. First of all, it is necessary to make the following assumptions.

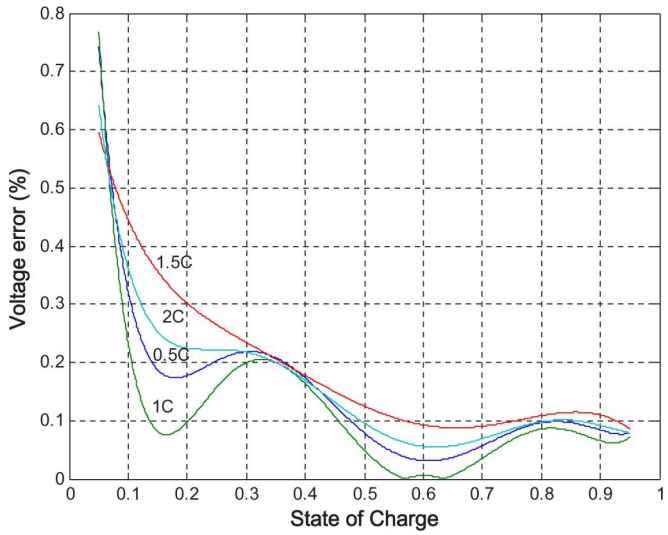

Fig. 10. Error of experiment data and the computed voltage at different charge currents.

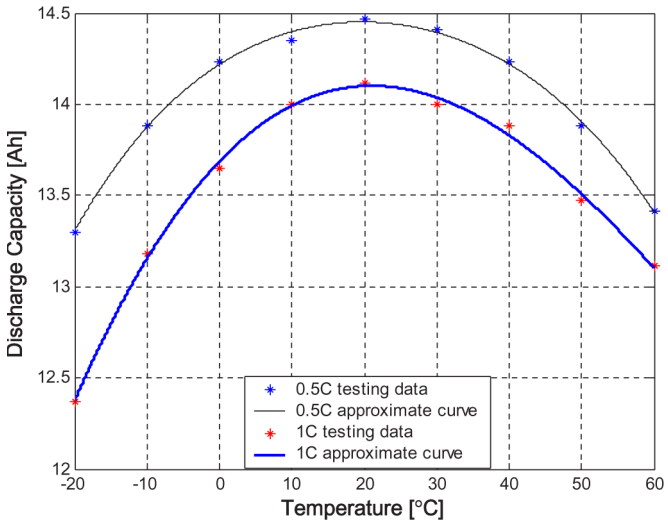

Fig. 11. Temperature dependence of the discharge capacity of the NiMH battery.

The considered battery is fully charged in nominal conditions: nominal current, nominal temperature, and nominal capacity ($i_b = 1$ C, $\tau_b = 20\,^{\circ}$C, and the capacity is designed for nominal parameters, respectively).

The EMF for the considered battery is defined as its nominal condition in the nominal SOC alteration range $k \in \langle 1, 0 \rangle$. The assumption is taken that the EMF value of $k = 0.15$ is the minimum EMF. For $k = 0$, the EMF is defined as the "minimum–minimorum" in practice, which should not be obtained. The same assumption is recommended for a value that is different from the nominal temperature for the k_τ (SOC) definition. As shown in Fig. 13, the starting point value of the EMF for a different value from the nominal temperature can be higher or lower, which means that the extension alteration of the SOC could be longer or shorter. For instance (see Fig. 11), in the case of the NiMH battery for a value that is higher than the nominal temperature, the discharge capacity is smaller than the nominal, which means that for a certain temperature, the battery capacity corresponding to this temperature is also

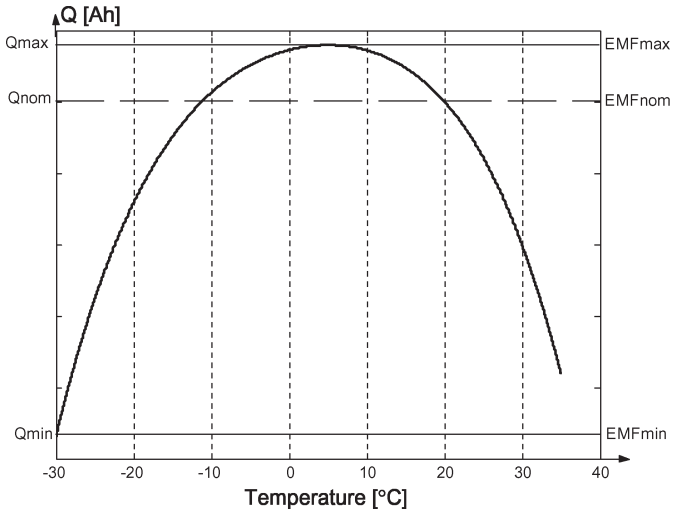

Fig. 12. Temperature dependence of the battery usable discharge capacity and the EMF starting point.

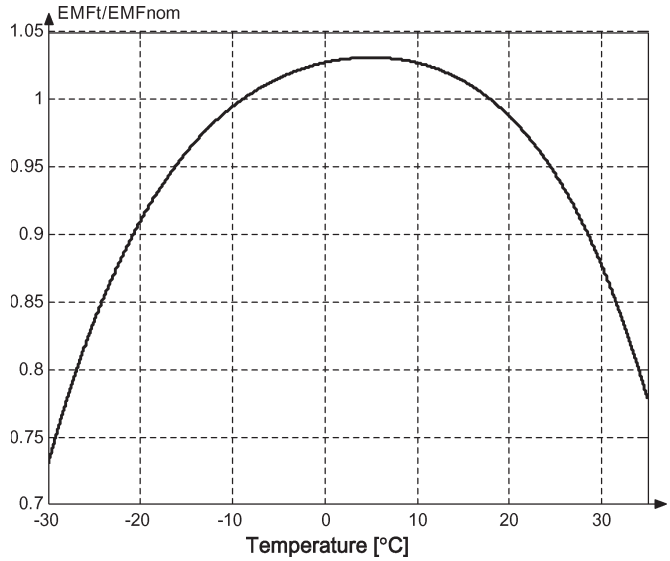

Fig. 13. Relation of $\mathrm{EMF}_\tau/\mathrm{EMF}_{\mathrm{nom}}$ and temperature.

changed in file $k_\tau \in \langle 1, 0\rangle$. However, the full k_τ does not mean the same discharge capacity as in the case of the nominal temperature but does mean the maximum discharge capacity at this temperature. For this reason, in fact, k_τ for this temperature is only $k(t) > k_\tau(t)$ [in some cases, $k(t) < k_\tau(t)$, where $k(t)$ is connected only with the nominal conditions].

From Fig. 12, it is easy to note that the EMF (in the case of this battery type) value in the nominal conditions is smaller than the EMF value for a temperature that is lower than 20 °C (the nominal temperature), which means that for a maximum EMF value, the available battery capacity is higher than in the case of the nominal terms. For nominal conditions, the SOC can be defined by a k factor ($k \in \langle 1, 0\rangle$). If the EMF for the nonnominal conditions reaches its highest value, the available charge (in ampere-hours) will be also greater. It is easy to note the relation $Q_\tau = Q_{\max}$, and Q_{nom} is defined as follows:

$$\frac{Q_\tau = Q_{\max}}{Q_{\mathrm{nom}}} > 1.$$

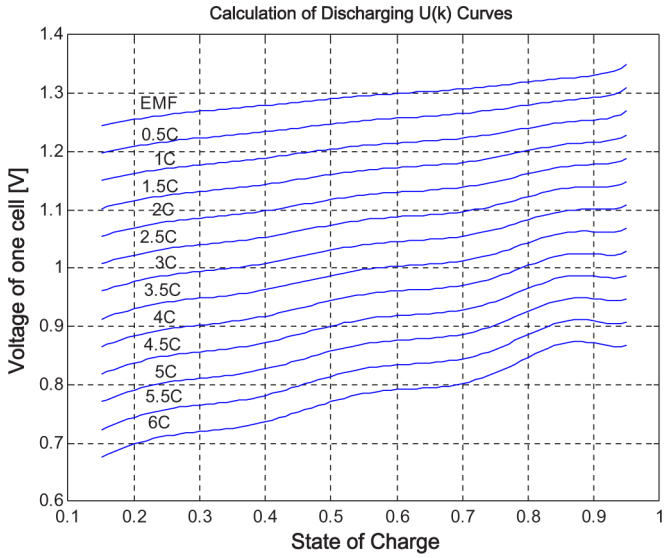

Fig. 14. EMF and calculated discharging voltage characteristics at different discharging current and nominal temperature.

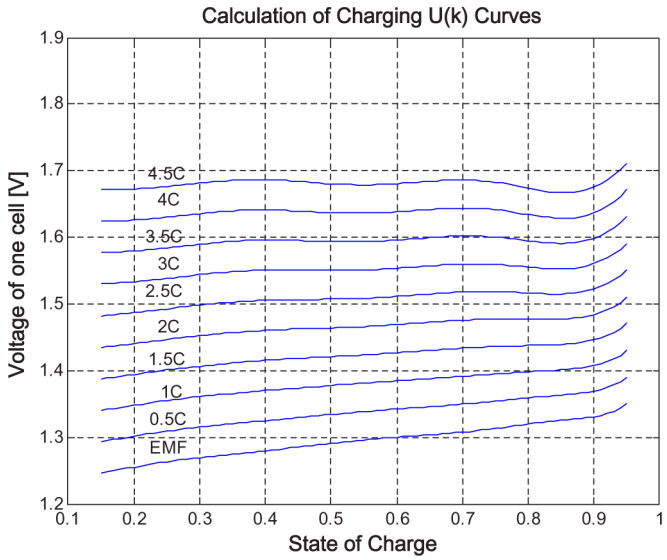

Fig. 15. EMF and calculated charging voltage characteristics at different charging current and nominal temperature.

[If $Q_\tau < Q_{\mathrm{nom}} \rightarrow (Q_\tau/Q_{\mathrm{nom}}) < 1$, correspondingly, $\mathrm{EMF}_\tau < \mathrm{EMF}_{\mathrm{nom}} \rightarrow (\mathrm{EMF}_\tau/\mathrm{EMF}_{\max}) < 1$.] This corresponds to $((\mathrm{EMF}_\tau = \mathrm{EMF}_{\max})/\mathrm{EMF}_{\mathrm{nom}}) > 1$. On the other hand, for Q_{nom}, $k \in \langle 1, 0\rangle$, but relating it to $Q_\tau > Q_{\mathrm{nom}}$ in τ condition, the file $\langle 1, 0\rangle$ means file $\langle 0, Q_{\max}\rangle$. Transforming k in nominal terms to k_τ is necessary to use the general relation $(Q_\tau/Q_{\mathrm{nom}})$. Theoretically, the product $k_{\mathrm{nom}}(Q_\tau/Q_{\mathrm{nom}})$ transfers the SOC factor into nominal temperature conditions. The same transformation can be obtained for $k_{\mathrm{nom}}(\mathrm{EMF}_\tau/\mathrm{EMF}_{\mathrm{nom}})$, where $k_{\mathrm{nom}} \in \langle 1, 0\rangle$.

Using the transformation factor $k_{\mathrm{nom}}(\mathrm{EMF}_\tau/\mathrm{EMF}_{\mathrm{nom}})$ or $k * s_\tau(k_{\mathrm{nom}} = k, s_\tau = (\mathrm{EMF}_\tau/\mathrm{EMF}_{\mathrm{nom}}))$, it is possible to relate the SOC of the battery that is determined for the nominal temperature to other different temperatures.

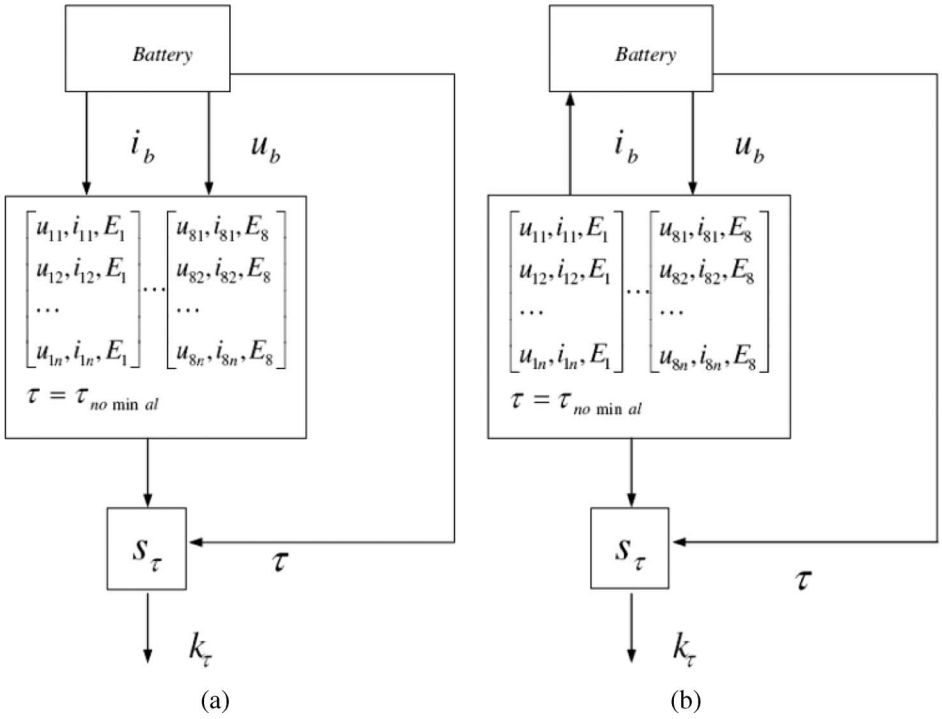

Fig. 16. SOC indication algorithm. (a) Discharging. (b) Charging.

V. Algorithm of Battery SOC Indication

The algorithm is given as follows.

1) By simulation, the family of $u_b(k)$ for different constant currents $i_b \in \langle 0.5\ \mathrm{C}, 6\ \mathrm{C} \rangle$ and nominal temperature (e.g., 20 °C) can be obtained according to battery modeling results (EMF and internal resistance as functions of the SOC).
2) From Fig. 13, $s_\tau = (\mathrm{EMF}_\tau / \mathrm{EMF}_{\mathrm{nom}})$ is defined for $\tau \in \langle -30\ ^\circ\mathrm{C}, +35\ ^\circ\mathrm{C} \rangle$.
3) From Fig. 14, for $k = 0.9, \ldots, 0.2$, the following lookup table can be obtained:

$$k = 0.9 \Rightarrow \begin{bmatrix} u_{11}, i_{11}, E_1 \\ u_{12}, i_{12}, E_1 \\ \vdots \\ u_{1n}, i_{1n}, E_1 \end{bmatrix} \cdots k = 0.2 \Rightarrow \begin{bmatrix} u_{81}, i_{81}, E_8 \\ u_{82}, i_{82}, E_8 \\ \vdots \\ u_{8n}, i_{8n}, E_8 \end{bmatrix}.$$

Because of the practical limitation of the SOC alteration of the battery that is applied in hybrid drives, the range of k changes can be expressed as $\langle 0.9, 0.2 \rangle$ for the nominal temperature.

4) Considering the real temperatures, the SOC of the battery in relation to the nominal temperature can be defined as $s_\tau * k = k_\tau$. For instance, at a temperature of $+5\,^\circ\mathrm{C}$, $(\mathrm{EMF}_\tau / \mathrm{EMF}_{\mathrm{nom}}) = 1.06$; hence, $k_{+5\,^\circ\mathrm{C}} = 1.06k$, which means that at this moment and this temperature, the available capacity is 1.06 times that of the nominal temperature. At a temperature of $+30\,^\circ\mathrm{C}$, $(\mathrm{EMF}_\tau / \mathrm{EMF}_{\mathrm{nom}}) = 0.89$; hence, $k_{+30\,^\circ\mathrm{C}} = 0.89k$, which means that at this moment and this temperature, the available capacity is 0.89 times that of the nominal temperature.

A similar method and process can be used for the battery charging process (see Fig. 15).

The above-depicted method can be used in the battery management system for the SOC "online" indication. Based on the aforementioned steps 1–4, the SOC indication algorithm can be depicted as in Fig. 16.

In practice, the battery SOC in HEVs changes not as deep and not as quickly as in pure electric vehicles, which means that the indication process may not be realized as frequently. It is not necessary to indicate the SOC of the battery every second; however, there will be no problem to indicate the SOC every minute for a microprocessor program using, for instance, properly prepared lookup tables of voltages, currents, and temperature factors. Certainly, the previous value of the SOC has to be remembered by a microprocessor.

VI. Conclusion

The assumed method and effective model are very accurate according to error checking results of the NiMH batteries from the Central Laboratory of Batteries and Cells. The modeling method is valid for different types of batteries. The model can be conveniently used for vehicle simulation because the battery model is accurately approximated by mathematical equations. The model provides the methodology for designing a battery management system and calculating the SOC. The influence of temperature on battery performance is analyzed according to laboratory-tested data, and the theoretical background for the SOC calculation is obtained. The algorithm of the battery SOC "online" indication considering the influence of temperature can be easily used in practice by a microprocessor.

REFERENCES

[1] K. L. Butler, M. Ehsani, and P. Kamath, "A Matlab-based modeling and simulation package for electric and hybrid electric vehicle design," *IEEE Trans. Veh. Technol.*, vol. 48, no. 6, pp. 1770–1778, Nov. 1999.

[2] O. Caumont, P. L. Moigne, C. Rombaut, X. Muneret, and P. Lenain, "Energy gauge for lead acid batteries in electric vehicles," *IEEE Trans. Energy Convers.*, vol. 15, no. 3, pp. 354–360, Sep. 2000.

[3] M. Ceraol and G. Pede, "Techniques for estimating the residual range of an electric vehicle," *IEEE Trans. Veh. Technol.*, vol. 50, no. 1, pp. 109–115, Jan. 2001.

[4] C. C. Chan, "The state of the art of electric and hybrid vehicles," *Proc. IEEE*, vol. 90, no. 2, pp. 247–275, Feb. 2002.

[5] V. H. Johnson and A. A. Pesaran, "Temperature-dependent battery models for high-power lithium-ion batteries," in *Proc. Int. Electr. Vehicle Symp.*, 2000, vol. 2, pp. 1–6.

[6] W. Gu and C. Wang, "Thermal–electrochemical modeling of battery systems," *J. Electrochem. Soc.*, vol. 147, no. 8, pp. 2910–2922, 2000.

[7] A. Szumanowski, *Fundamentals of Hybrid Vehicle Drives*. Warsaw, Poland: Warsaw-Radom, 2000. Monograph Book.

[8] A. Szumanowski, *Hybrid Electric Vehicle Drives Design—Edition Based on Urban Buses*. Warsaw, Poland: Warsaw-Radom, 2006. Monograph Book.

[9] R. F. Nelson, "Power requirements for battery in HEVs," *J. Power Sources*, vol. 91, pp. 2–26, 2000.

[10] E. Karden, S. Buller, and R. W. De Doncker, "A frequency-domain approach to dynamical modeling of electrochemical power sources," *Electrochim. Acta*, vol. 47, no. 13/14, pp. 2347–2356, 2002.

[11] J. Marcos, A. Lago, C. M. Penalver, J. Doval, A. Nogueira, C. Castro, and J. Chamadoira, "An approach to real behaviour modeling for traction lead-acid batteries," in *Proc. Power Electron. Spec. Conf.*, 2001, vol. 2, pp. 620–624.

[12] A. Salkind, T. Atwater, P. Singh, S. Nelatury, S. Damodar, C. Fennie, and D. Reisner, "Dynamic characterization of small lead-acid cells," *J. Power Sources*, vol. 96, no. 1, pp. 151–159, 2001.

[13] G. Plett, "LiPB dynamic cell models for Kalman-filter SOC estimation," in *Proc. Int. Electr. Vehicle Symp.*, 2003. [CD-ROM].

[14] S. Pang, J. Farrell, J. Du, and M. Barth, "Battery state-of-charge estimation," in *Proc. Amer. Control Conf.*, 2001, vol. 2, pp. 1644–1649.

[15] S. Malkhandi, S. K. Sinha, and K. Muthukumar, "Estimation of state of charge of lead acid battery using radial basis function," in *Proc. Ind. Electron. Conf.*, 2001, vol. 1, pp. 131–136.

[16] S. Rodrigues, N. Munichandraiah, and A. Shukla, "A review of state-of-charge indication of batteries by means of a.c. impedance measurements," *J. Power Sources*, vol. 87, no. 1/2, pp. 12–20, 2000.

[17] L. Jyunichi and T. Hiroya, "Battery state-of-charge indicator for electric vehicle," in *Proc. Int. Electr. Vehicle Symp.*, 1996, vol. 2, pp. 229–234.

[18] S. Sato and A. Kawamura, "A new estimation method of state of charge using terminal voltage and internal resistance for lead acid battery," in *Proc. Power*, 2002, vol. 2, pp. 565–570.

[19] W. X. Shen, C. C. Chan, E. W. C. Lo, and K. T. Chau, "Estimation of battery available capacity under variable discharge currents," *J. Power Sources*, vol. 103, no. 2, pp. 180–187, 2002.

[20] W. X. Shen, K. T. Chau, C. C. Chan, and E. W. C. Lo, "Neural network-based residual capacity indicator for nickel-metal hydride batteries in electric vehicles," *IEEE Trans. Veh. Technol.*, vol. 54, no. 5, pp. 1705–1712, Sep. 2005.

[21] K. Morio, H. Kazuhiro, and P. Anil, "Battery SOC and distance to empty meter of the Honda EV plus," in *Proc. Int. Electr. Vehicle Symp.*, 1997, pp. 1–10.

[22] O. Caumont, P. L. Moigne, C. Rombaut, X. Muneret, and P. Lenain, "Energy gauge for lead-acid batteries in electric vehicles," *IEEE Trans. Energy Convers.*, vol. 15, no. 3, pp. 354–360, Sep. 2000.

[23] S. Piller, M. Perrin, and A. Jossen, "Methods for state-of-charge determination and their applications," *J. Power Sources*, vol. 96, no. 1, pp. 113–120, Jun. 2001.

[24] A. Szumanowski, J. Dêbicki, A. Hajduga, P. Piórkowski, and C. Yuhua, "Li-ion battery modeling and monitoring approach for hybrid electric vehicle applications," in *Proc. Int. Electr. Vehicle Symp.*, 2003. [CD-ROM].

Antoni Szumanowski received the M.Sc., Ph.D., and D.Sc. degrees from Warsaw University of Technology (WUT), Warsaw, Poland, in 1970, 1978, and 1985, respectively.

From 1984 to 1993, he was a Professor nominated by WUT. In 1993, he was a Professor nominated by the President of the Republic of Poland. Since 2001, he has been a Professor (the highest level) nominated by Polish Ministry of Education. He is currently with the WUT. He has been involved in research on HEVs since 1976. He has published five monographs and books in Polish in the field of HEVs and energy storage systems–alternative energy sources and two monographs in English—*Fundamentals of Hybrid Vehicle Drives* [Warsaw-Radom, Poland, National Research Institute (NRI), 2000] and *Hybrid Electric Vehicle Drives Design Edition Based on Urban Buses* (Warsaw-Radom, Poland, NRI, 2006). He is the holder of more than 20 patents, the majority of them in the field of HEVs.

Prof. Szumanowski is a Board Member of the European Association for Battery, Hybrid, and Fuel Cell Electric Vehicles (AVERE) and the President of Polish Association for Ecological Vehicles, which is a branch of AVERE. He is a member of the Scientific Council Boards of the Polish Science and Technology Institutes. He is also a member of the Committee of the Electric Vehicle Symposium since 1999.

Yuhua Chang received the M.Sc. and Ph.D. degrees from Warsaw University of Technology (WUT), Warsaw, Poland, in 2005 and 2007, respectively.

Since 2003, she has been a Research Assistant of Prof. A. Szumanowski in the field of battery modeling and management in HEVs and the configuration design of a propulsion system for HEVs by simulation. She is currently a member of the faculty of WUT.